Biased domain walls

D. Coulson
D. Rittenhouse Laboratory, University of Pennsylvania, Philadelphia, Pennsylvania 19104

Z. Lalak
D. Rittenhouse Laboratory, University of Pennsylvania, Philadelphia, Pennsylvania 19104
and Institute of Theoretical Physics, University of Warsaw, Warsaw, Poland 00-681

B. Ovrut
D. Rittenhouse Laboratory, University of Pennsylvania, Philadelphia, Pennsylvania 19104
(Received 20 July 1995)

Domain walls form naturally in the early Universe whenever a discrete symmetry is spontaneously broken at some phase transition. When each vacuum is populated equally, it is well known that the domain wall network comes to dominate the energy density of the Universe and causes excessive anisotropy in the cosmic microwave background. We present results for the initial conditions and dynamical evolution of domain wall networks in which one of the degenerate vacua has a population bias over the other. The initial distribution of domain walls is well described by percolation theory. We find that such networks, although they show evidence of a limited scaling regime for a range of biases, do not persist indefinitely. It follows that biased domain wall networks avoid the energy density and anisotropy problems.

PACS number(s): 98.80.Cq, 11.27.+d, 98.65.Dx

I. INTRODUCTION

Topological defects provide cosmologists with a set of intriguing mechanisms for structure formation which are quite different in nature to the standard inflationary paradigm [1]. Defects form at spontaneous symmetry breaking phase transitions in the early Universe, and their subsequent field ordering dynamics can perturb the matter and radiation content of the Universe, leaving characteristic signals in both the present day matter distribution and the microwave background.

The nature of the defect is determined by the topology of the vacuum manifold following the phase transition. A $\mathscr{Z}_2$ manifold with two disconnected vacua leads to domain walls [2], an $\mathscr{S}^1$ manifold to cosmic strings [3], an $\mathscr{S}^2$ manifold to monopoles, and an $\mathscr{S}^3$ manifold to cosmological texture [4]. Much recent attention has focused on the gauged cosmic string [5], and global texture scenarios [6]. However, even though discrete symmetries arise naturally in many particle physics models, cosmological domain walls have long been considered unworkable. Zel'dovich, Kobzarev, and Okun noticed in 1975 that the energy density of a domain wall network will eventually come to dominate that of matter or radiation. More recent attempts to save domain wall scenarios, such as the the so-called ''late-time'' phase transitions [7], are now known to be in conflict with observations of the microwave background [8,9], and suffer other serious problems [11].

The most complete study of the dynamics of domain wall networks was given by Press, Ryden, and Spergel [9]. These authors studied the time evolution, during the era of matter domination, of topological domain wall kinks in a scalar field with a potential energy possessing two minima, both degenerate in energy. They showed conclusively that such networks rapidly evolved into long domain walls stretching across the Universe whose surface area, and, hence energy density, persisted for a long time. This persistence, or scaling behavior, led both to the relatively rapid domination of the energy density of the universe by these walls and to large distortions in the cosmic microwave background. Both of these results are incompatible with observations.

It did appear therefore that domain walls could not have formed in the early Universe. However, these results were based on specific, and apparently reasonable, assumptions about the initial conditions of the domain wall network. To be precise, these authors initialized their networks by allowing the computer to randomly choose, at any point on the lattice, either one vacuum state or the other *with each vacuum weighted with equal probability*. Furthermore, the choice of the vacuum state was completely uncorrelated from one lattice site to another.

As is well known, such an initial distribution on a lattice can be described statistically using percolation theory [12]. On a three-dimensional square lattice, there is a critical probability, $p_c = 0.311$, above which the associated vacuum will percolate across the entire lattice. It is easy to see that, by initializing both vacua with a probability $p = 1/2$, both vacua must propagate across the lattice. Since domain walls lie on the interface between the two different vacua, this means that enormous domain walls must form which extend across the entire Universe. This gives a clear mathematical explanation for the Press, Ryden, and Spergel result. However, if for some reason the two vacua were to be given different, or biased, probabilities, then these conclusions could be dramatically altered. For example, if one vacuum had $p < p_c$, then that vacuum would form finite clusters in the percolating sea of the other vacuum. The domain walls would then be small, finite bags whose dynamics would undoubtedly be very different. In particular, such small domain walls would

probably disappear relatively rapidly, thus avoiding the two problems associated with infinitely long walls.

Furthermore, it has become clear in recent years that nonequilibrium phase transitions, which can occur in realistic models of the early Universe, generically lead to a biased choice of vacuum state. There seems to be every reason then to restudy the classic work of Press, Ryden, and Spergel with the modification that the domain wall network be initialized using biased vacuum probabilities. That is the main aim of this paper.

This paper is organized as follows. Section II discusses the nature of the domain wall network immediately following a cosmological phase transition. We will use percolation theory to explain the radically different topologies of the networks in two and three dimensions, and for small and large bias probabilities, p. In Sec. III, the dynamical evolution of the domain wall networks is discussed. We present a semianalytic argument for the lack of persistence of any domain wall network in the case $p \neq 1/2$, and consider the details of numerically implementing the scalar field equation of motion. Results are given in Sec. IV for the two- and three-dimensional computer simulations, while in Sec. V we discuss these results and give concluding remarks.

II. INITIAL CONDITIONS

The initial conditions of the scalar field network immediately following a cosmological phase transition depend on the nature of the post-transition vacuum manifold. We will consider the case in which the scalar field potential has just two disconnected minima which we will refer to as the $(+)$ vacuum and the $(-)$ vacuum, respectively. At the phase transition, the field has some finite correlation length (like the inverse Ginzburg temperature in case of a transition triggered by thermal fluctuations) over which the post-transition vacuum is chosen coherently. We will denote this length by Λ. One can approximate the initial spatial structure of the vacuum produced during the transition by first dividing space into cells of volume Λ^d, where d is the dimension, and second, by assuming that choices of the new vacua are made independently in each cell, giving the $(+)$ vacuum with probability p and the $(-)$ vacuum with probability $1-p$, where $0 \leqslant p \leqslant 1/2$. (Note, there is clearly a symmetry $p \rightarrow 1-p$. However, for clarity we *define* the $(+)$ vacuum to be that with a population bias $\leqslant 1/2$.) Whenever the vacua in neighboring cells are different, a domain wall will form which interpolates between them, and so, typically, a complicated spatial network of domain walls will form.

If a phase transition is triggered by fluctuations in a system in thermal equilibrium, one expects the ratio $p/(1-p)$ to be $p/(1-p) = \exp(-E_+/T)/\exp(-E_-/T)$, where $E_{+,-}$ are the energies of the local vacua. Hence, if the vacua are truly degenerate, then the probability must take the value $p = 1/2$. However, in this paper we will consider the case of a more generic phase transition in which, although the two vacua are degenerate, the population probabilities of each need not be equal. That is, in general $p \neq 1/2$. Clearly, such transitions can only occur in a system that is too weakly coupled to achieve thermal equilibrium. We will refer to these as nonequilibrium or biased phase transitions. A number of such biased transitions have recently been investigated, such as those occurring in very light scalar fields in deSitter space [13,14]. We will not pursue the theoretical aspects of these biased transitions in this work. Rather, we shall investigate the nature of the initial domain wall network formed during biased phase transitions, and then present a detailed study of its subsequent dynamical evolution.

Of course, an arbitrary spatial superposition of domain walls, such as that produced by the mechanism described above, is not a solution of the equations of motion and cannot be stable. However, such a superposition represents physical initial conditions, the subsequent evolution of which is governed by the dynamics of the theory. Subject to this dynamics, the initially static domain walls acquire nonzero velocities, oscillate under their surface tension, and interact with one another.

In the most authoritative study of domain wall network evolution to date [9], the authors concentrate exclusively on the example of the ''equilibrium network,'' with no bias of one vacuum over the other. In their work, each lattice site was initialized with a random value of the field drawn from a uniform distribution between $-\phi_0$, the $(-)$ vacuum, and $+\phi_0$, the $(+)$ vacuum. However, after a short time, these results become indistinguishable from randomly initializing the scalar field to be only $-\phi_0$ or $+\phi_0$, each with probability $p = 1/2$. These authors set the initial velocity of the domain walls to zero.

In this paper, we concentrate on the example of the ''biased network.'' We initialize the scalar field by randomly setting it equal to $-\phi_0$ or $+\phi_0$ at each lattice site, with bias probability p for $+\phi_0$ and $1-p$ for $-\phi_0$ with $0 \leqslant p \leqslant 1/2$. Thus, our lattice resolution corresponds to the initial field correlation length, and on physical scales above the resolution cutoff the field will have a white noise power spectrum; that is, there are no field correlations from one lattice site to another. With this choice of initial conditions, the pattern of vacua which appears on the lattice corresponds to that predicted by percolation theory. (We discuss the generalization to more continuously distributed initial conditions below.)

Percolation theory predicts statistical characteristics and topological properties of a ''typical'' vacuum pattern formed on the lattice [12]. In the subsequent sections of this paper we will investigate the connection between the initial conditions predicted by percolation theory and the behavior of the dynamically evolving biased networks. To set the language and to establish notational conventions we will first briefly discuss some of the relevant results from percolation theory.

Percolation theory tells us that for a given lattice there exists some critical probability, p_c. If the population probability for a given vacuum exceeds this critical value, that vacuum will percolate the lattice; that is, one can trace a path from one face of the lattice to another without crossing a domain wall (a scalar field zero isosurface). If the bias probability of a vacuum is less than the critical value, however, that vacuum will not percolate, and domain wall ''bags,'' or clusters, of this vacuum will form. Whether one, both, or neither vacua percolate depends on the spatial dimension and the relative values of p, $1-p$, and p_c.

It has been shown that $p_c = 0.311$ is the critical probability for a cubic lattice in three dimensions [15]. Thus, for $p < p_c$, the $(+)$ vacua are in finite clusters while the $(-)$ vacua sites lie predominantly in a large percolating cluster,

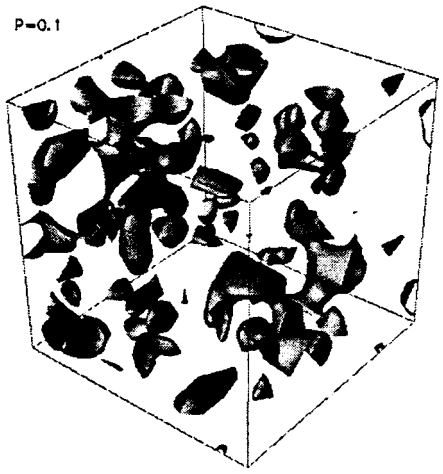

FIG. 1. Initial distribution of domain walls in three dimensions with bias probability, $p=0.1$. Here we show a $(10\Lambda)^3$ grid.

since necessarily $1-p>p_c$. It follows that the associated domain walls are relatively small, forming around the compact boundaries of the finite clusters. Figure 1 shows this behavior in the case of a small bias probability, $p=0.1<p_c$. Note that there exist only finite, disconnected domain wall bags, the number and size of which can be shown to grow as p approaches p_c from below. For the case that both p and $1-p$ exceed p_c, both vacua will percolate the lattice, and infinite (that is, lattice sized) domain walls separating the vacua will form. A small number of domain wall bags, disconnected from the percolating cluster, also form but their number decreases as p approaches 0.5. Figure 2 shows this ''infinite'' domain wall structure in the limiting case of $p=0.5$. The crucial lesson to be learned from all this is that in three dimensions, when both vacua percolate, as in the $p=0.5$ case discussed in [3], the topology of the post-transition vacuum is one of long, convoluted domain walls stretching across all space, whereas, when $p<p_c$, the vacuum is composed of small, compact domain wall bags.

In two dimensions, the critical probability for a square

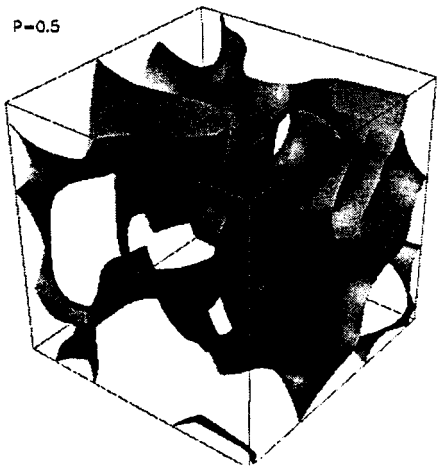

FIG. 2. Initial distribution of domain walls in three dimensions with bias probability, $p=0.5$. For clarity we show here only a $(5\Lambda)^3$ grid.

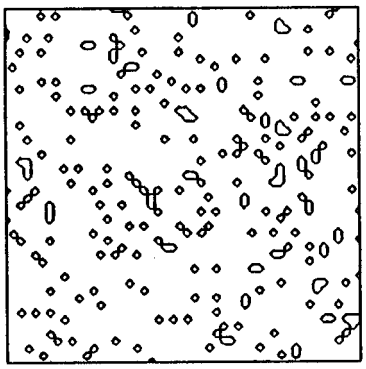

FIG. 3. Initial distribution of domain walls in two dimensions with bias probability, $p=0.1$. Here we show a $(50\Lambda)^2$ grid.

lattice is $p_c=0.593$. This substantially changes some features of the domain wall network. For $p<1-p_c=0.407$, the $(+)$ vacua lie in finite clusters surrounded by a sea of predominately percolating $(-)$ vacua. The associated domain walls are, therefore, in the form of small compact bags. This behavior is clearly seen in Fig. 3 where we choose $p=0.1<1-p_c$. Domain walls of this type also occurred in three dimensions, as we have seen. However, unlike the three-dimensional case, there is now a range of p given by $1-p_c=0.407\leqslant p\leqslant p_c=0.593$, where neither vacuum percolates. The vacuum structure in this case is a complicated mesh of domain walls, similar to a fishing net. This netlike behavior is clearly visible in Fig. 4 where we present the $p=0.5$ case. As one can easily convince oneself, neither vacuum percolates. There are only finite clusters of each vacuum, surrounded by finite walls. It is impossible to go from one edge of the figure to the opposite one remaining in one vacuum only.

Finally, we note that, unlike the case in three dimensions, it is never possible to have two simultaneously percolating vacua. It follows that long, convoluted domain walls stretching across all space can never occur in two dimensions. The crucial lesson to be learned is that when neither vacua percolates, such as in the $p=0.5$ case, a dense netlike structure of domain walls form, whereas, when $p<0.407$, the vacuum is composed of small, compact domain wall bags. The critical threshold is visible as a growth of the number of bubbles

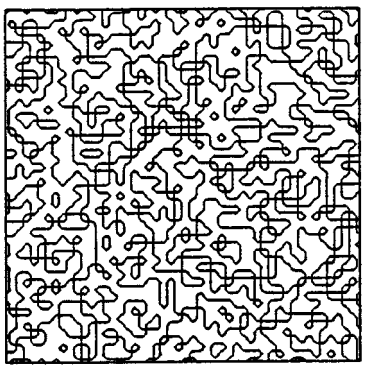

FIG. 4. Initial distribution of domain walls in two dimensions with bias probability, $p=0.5$. Here we show here a $(50\Lambda)^2$ grid.

of the less probable component as p approaches $1-p_c$ until, at $p=1-p_c$, these bubbles all touch and percolation ceases.

Percolation theory allows one to give a reasonably accurate mathematical description of the number of finite s clusters, their radius and the size of their boundary. Here s denotes the number of neighboring lattice sites that are occupied by the same vacuum. Let n_s be the probability that a given lattice site is an element of an s cluster. This is a fundamental quantity, given by the ratio of the total number of s clusters over the total number of lattice sites. An analytical expression for this quantity has been found in both two and three dimensions [13], using scaling arguments and Monte Carlo simulations. For example, the result in $d=3$ is given by

$$n_s=0.0501s^{-\tau}\exp\left\{-0.6299\left(\frac{p-p_c}{p_c}\right)\times s^{\sigma}\left[\left(\frac{p-p_c}{p}\right)s^{\sigma}+1.6679\right]\right\}, \tag{1}$$

where $\tau=2.17$ and $\sigma=0.48$. Similarly, in three dimensions, the average radius of gyration for an s cluster $R_s(p)$, for $p<p_c$ and $s>s_\xi$, is found to be

$$R_s(p)=0.702(p_c-p)^{0.322}s^{0.55}\Lambda, \tag{2}$$

where

$$s_\xi=\left(\frac{0.311}{|p-0.311|}\right)^{2.08}. \tag{3}$$

It can also be shown, for $p<p_c$ and $s\gtrsim 5$, that every s cluster has a boundary composed of

$$t_s=\left(\frac{1-p}{p}\right)s \tag{4}$$

sites. One can easily check using the formula for n_s that, on a given lattice, the number of s clusters falls rather quickly with growing s. Hence there is an $s_{\max}$ such that the total number of $s_{\max}$ clusters is 1. In other words, formation of clusters with s much larger than $s_{\max}$ is extremely improbable. This means that on a given lattice there exists an upper statistical cutoff on the size of observable clusters. Clearly, the mathematical details of percolation theory lie outside the region of study in this paper. We refer the reader to [13], and particularly to its Appendix, for details.

Using the above formulas, as well as other results found in [13], it is possible, for a fixed lattice and a given value of p, to compute the surface area for the domain walls between the $(+)$ and the $(-)$ vacua. In particular, we have attempted to compute the domain wall surface area for the three dimensional cubic lattice case. However, this calculation is very difficult when there are two percolating vacua and hence, we are restricted to a calculation for $p<p_c$. This difficulty arises from the fact that the associated large domain walls are highly fractalized and hence their surface area is difficult to characterize. Also, the finite size of the lattice leads to the phenomenon of a preincipient cluster, essentially two percolating clusters, even for p somewhat below p_c. We find that we can perform a reasonable calculation only for $p\lesssim 0.25$.

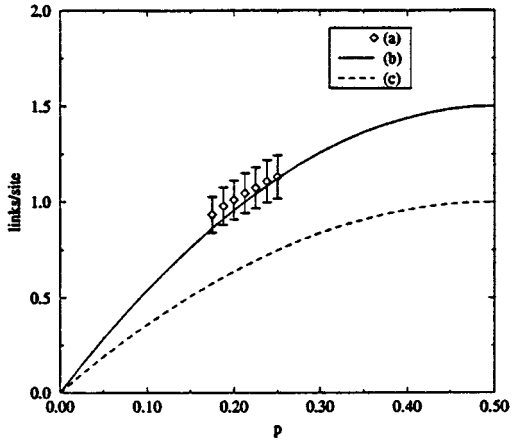

FIG. 5. The number of links across which a domain wall falls per lattice site. Points (a) are the $3d$ percolative predictions in the regime $0.175\leqslant p\leqslant 0.25$, with their associated uncertainty ($\sim 10\%$). Line (b) shows the measured values (averaged over 20 three-dimensional samples) for $0\leqslant p\leqslant 0.5$. Line (c) shows the analogous curve in two dimensions. Error bars on both curves are too small to show.

Furthermore, formula (1) for n_s is not very accurate for $p<0.175$. This puts a lower bound on the calculation. A very reasonable calculation can be performed in the range $0.175\leqslant p\leqslant 0.25$ but, even in this range, we estimate an error of about 10%. All of the information necessary to carry out this calculation can be found in [13] and we will not repeat this work here. Our results for the domain wall surface area are plotted, along with the 10% error bars, as curve (a) in Fig. 5.

These results can be checked, and extended to any values of p, simply by letting the computer evaluate wall surface area. The solid line (b) in Fig. 5 represents the mean initial surface area of ten three-dimensional realizations generated for $0\leqslant p\leqslant 0.5$. The initial area grows monotonically with p, approaching the maximal value of $1.5\times V$ at $p=0.5$. Note that in the region where we can compare the percolation prediction with the computer experiment, there is good agreement. The growth of the area above p_c demonstrates that above the threshold the area is totally dominated by the area of the percolating cluster, which must be highly fractalized, since one can easily check that the surface of small clusters tends to vanish with rising p. The line (c) in Fig. 5 shows the initial surface area in two dimensions. Both curves, (b) and (c), are smooth in the vicinity of the percolation thresholds. That is, there is no detectable change in the character of the curves at criticality. This is a surprising observation, as one would think naively that the percolation threshold should be visible in important quantities, like the surface area. However, on a finite lattice, this is not too surprising. As mentioned above, as p approaches p_c on a finite lattice, a preincipient cluster begins to grow, starting out very small but growing continuously until it becomes a percolating cluster at the critical threshold. It follows that the surface area will grow continuously even when passing through the p_c threshold, as observed. The lesson we learn from this is that, even though the topology of the domain walls changes from compact bags to long walls as p becomes larger than

p_c, this is not seen as a discontinuous change in the wall surface area when computed on a finite lattice.

In this section we have discussed the important features of the initial conditions which we will use in our analysis of the evolution of the biased domain wall networks in two and three dimensions. The role of dynamics in propagating or erasing these initial conditions is presented, in detail, in the following section.

III. EVOLUTION

To investigate the dynamical evolution of the initial conditions described above, we choose to follow Press, Ryden, and Spergel (PRS) [9]. The dynamics of the scalar field, ϕ, are determined by the equation of motion

$$\frac{\partial^2\phi}{\partial\eta^2}+\frac{2}{\eta}\frac{d\ \ln a}{d\ \ln\eta}\frac{\partial\phi}{\partial\eta}-\nabla^2\phi=-a^2\frac{\partial V}{\partial\phi}, \tag{5}$$

where η is the conformal time coordinate, a is the scale factor of the Universe ($a\sim\eta$ in the radiation era, and $a\sim\eta^2$ in the matter era), V is the scalar potential, and the spatial gradients are with respect to comoving coordinates. The scalar potential determines the topology of the vacuum manifold. We choose a generic ϕ^4 potential

$$V(\phi)=V_0\left(\frac{\phi^2}{\phi_0^2}-1\right)^2 \tag{6}$$

with the two degenerate vacua, $\phi=\pm\phi_0$, separated by a potential barrier V_0.

Following PRS we can define a physical domain wall thickness w_0 given by

$$w_0\equiv\pi\frac{\phi_0}{\sqrt{2V_0}}. \tag{7}$$

The ratio of the wall thickness to the horizon size ($\mathscr{H}^{-1}=[(1/a)(\partial a/\partial\eta)]^{-1}$) at the time of the phase transition

$$W_0\equiv\frac{w_0}{a(\eta_0)}\frac{1}{\eta_0}\frac{d\ \ln a}{d\ \ln\eta}\bigg|_{\eta_0} \tag{8}$$

then sets η_0, the conformal time of the phase transition and the time at which we begin the simulation.

Before considering the numerical evolution of this equation of motion, let us consider the nature of the solutions of such a system. The choice of a quartic potential (6) means the equation of motion of the scalar field is nonlinear, and hence analytically quite intractable. However, the formation of domain walls is guaranteed whenever the vacuum manifold has a $\mathscr{Z}_2$ symmetry, so we can consider any potential with two degenerate minima. The piecewise quadratic potential

$$V(\phi)=\begin{cases}V_0\left(1-2\dfrac{\phi^2}{\phi_0^2}\right), & |\phi|<\phi_0/2,\\ 2\dfrac{V_0}{\phi_0^2}(|\phi|-\phi_0)^2, & |\phi|>\phi_0/2,\end{cases} \tag{9}$$

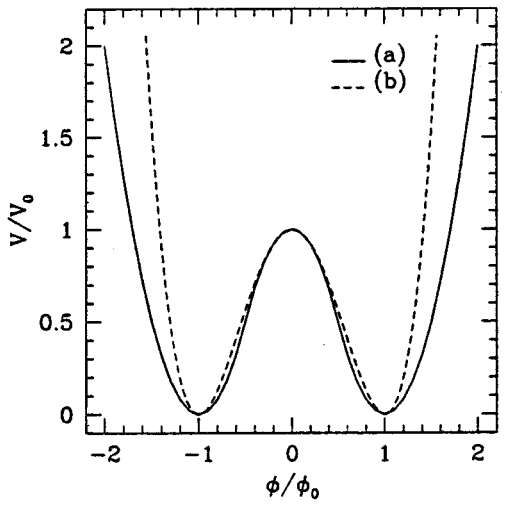

FIG. 6. A comparison of the piecewise-quadratic (a) and quartic (b) potentials, the exact expressions for which are given in Eqs. (9) and (6), respectively.

where $\phi_0\geqslant 0$, is particularly useful since the associated equation of motion is linear. A comparison of this potential with the original potential given in Eq. (6) is shown in Fig. 6. Note that in the region of interest, $-\phi_0\leqslant\phi\leqslant\phi_0$, these potentials are nearly equivalent. Henceforth, we will use the quadratic potential (9). Decomposing the scalar field into its Fourier modes, ϕ_k, we find that the equation of motion for each k mode is independent, and is given by

$$\frac{\partial^2\phi_k}{\partial\eta^2}+\frac{2}{\eta}\frac{d\ \ln a}{d\ \ln\eta}\frac{\partial\phi_k}{\partial\eta}+k^2\phi_k=-a^2\frac{\partial V}{\partial\phi}\bigg|_k\equiv-a^2\frac{\partial V(\phi_k)}{\partial\phi_k}, \tag{10}$$

where the final equivalence is valid for at most quadratic potentials. Note that in such a case, the potential term for each mode has the same functional form.

As discussed above, the initial conditions of the scalar field are described by percolation theory and correspond to a white noise power spectrum. It follows that the Fourier modes are excited with equal power on all scales (up to some cutoff, $k=K$, corresponding to the field correlation scale at the phase transition, Λ). Specifically, the Fourier modes, for $k\neq 0$, can be written as

$$\phi_k(\eta_0)=Ae^{i\theta_k}, \tag{11}$$

where θ_k is some weighted random phase. Since

$$\langle\phi^2\rangle=\frac{1}{\mathscr{V}}\int_\Lambda d\mathbf{x}\ \phi(\mathbf{x})\phi(\mathbf{x}) \tag{12}$$

$$=\int^K d\mathbf{k}\ \phi(\mathbf{k})\phi(\mathbf{k})^* \tag{13}$$

$$=\phi_0^2, \tag{14}$$

where $\mathscr{V}$ is the spatial volume, we see that coefficient A is simply related to the initial mean square value of the scalar

field distribution [for example, in the one-dimensional (1D) case, $A=\sqrt{\phi_0^2/K}$]. The zero mode is determined by the bias probability p,

$$\phi_{(k=0)}(\eta_0)=\langle\phi(\eta_0)\rangle=(2p-1)\phi_0, \tag{15}$$

giving the variance $\Delta=\langle\phi^2\rangle-\langle\phi\rangle^2$ of the initial scalar field distribution as

$$\Delta(\eta_0)=4p(1-p)\phi_0^2. \tag{16}$$

Following the phase transition, each mode evolves according to Eq. (10). Eventually, the potential term of this equation will come to dominate the gradient term for all k ($<K$), and each mode will be forced to a potential minimum $\pm\phi_0$, the sign of which will depend on the initial phase of the mode θ_k. Note, however, that $\langle\phi^2\rangle$ will remain approximately equal to ϕ_0^2 for any value of η. Similarly, if the zero mode is initially nonzero it will also roll to one or the other of the $\pm\phi_0$ minima of the potential, depending on its initial value given in Eq. (15).

Let us first consider the special case of $p=1/2$. The initial zero mode is just

$$\phi_{(k=0)}(\eta_0)=\langle\phi(\eta_0)\rangle=0. \tag{17}$$

This is an unstable equilibrium point of the potential. Thus in this special case, the zero mode will not be excited ($\langle\phi\rangle=0$ for all η), and

$$\Delta(\eta)\simeq\phi_0^2 \tag{18}$$

for all values of η. Hence, the network of domain walls separating the two vacua will persist indefinitely.

For $p\neq1/2$, the initial zero mode is nonvanishing at the phase transition, $\phi_{(k=0)}(\eta_0)\neq0$. Thus, the evolution will force the average field value to

$$\langle\phi\rangle=\phi_{(k=0)}\rightarrow\mathrm{sgn}[\phi_{(k=0)}(\eta_0)]\phi_0, \tag{19}$$

and the variance will tend to zero:

$$\Delta\rightarrow0. \tag{20}$$

In this case then, the scalar field will migrate to one of the (degenerate) vacua everywhere in space, and any initial network of domain walls will necessarily have only a finite effective lifetime.

So, we have seen that at least in the case of the analytically tractable quadratic potential, the evolution of the domain wall network depends sensitively on the initial conditions. For the case $p=0.5$, we expect the network of domain walls to persist indefinitely, while for $p\neq0.5$, one of the degenerate vacua will always come to dominate the other.

This analysis depends on the linearity of the equation of motion. For the case of the more generic quartic potential, nonlinear effects also have to be taken into account, which we do in the numerical experiments described below. However, the general feature of the domination of one vacuum over the other in the $p\neq1/2$ cases is expected to follow, as indeed our results show.

We now consider the somewhat problematic numerical implementation of Eq. (5). The physical thickness of a domain wall is constant, and so in comoving coordinates it decreases as a^{-1}. Thus on any reasonably sized comoving grid it proves impossible to ensure the walls remain resolved through to the end of a calculation (when the horizon size is roughly the lattice size). However, once formed and well separated, the walls' dynamics must be independent of their physical thickness. So to avoid this numerical problem we consider a generalization of Eq. (5) which forces the walls to maintain a constant comoving thickness while otherwise not altering their dynamics. This modified equation of motion becomes

$$\frac{\partial^2\phi}{\partial\eta^2}+\frac{\alpha}{\eta}\frac{d\ \ln a}{d\ \ln\eta}\frac{\partial\phi}{\partial\eta}-\nabla^2\phi=-a^\beta\frac{\partial V}{\partial\phi}. \tag{21}$$

Here, $\alpha=\beta=2$ which reproduces Eq. (5) will be replaced with $\alpha=3$, $\beta=0$. We refer the reader to PRS for a full justification of this change, and below present two arguments in support of this assumption. (An alternative algorithm for domain wall evolution, assuming infinitely thin domain walls is discussed elsewhere [10].)

We evolve Eq. (21) on a regular Cartesian grid with periodic boundary conditions; simulations are performed in two and three dimensions. Our finite difference scheme is second order accurate in both space and time, with the lattice equations:

$$\delta\equiv\frac{1}{2}\alpha\frac{\Delta\eta}{\eta}\frac{d\ \ln a}{d\ \ln\eta}, \tag{22}$$

$$(\nabla^2\phi)_{i,j,k}\equiv\phi_{i+1,j,k}+\phi_{i-1,k,k}+\phi_{i,j+1,k}+\phi_{i,j-1,k}+\phi_{i,j,k+1}+\phi_{i,j,k-1}-6\phi_{i,j,k}, \tag{23}$$

$$\dot\phi_{i,j,k}^{n+1/2}=\frac{(1-\delta)\dot\phi_{i,j,k}^{n-1/2}+\Delta\eta[\nabla^2\phi_{ijk}^n-a^\beta(\partial V/\partial\phi_{ijk}^n)]}{1+\delta}, \tag{24}$$

$$\phi_{i,j,k}^{n+1}=\phi_{i,j,k}^n+\Delta\eta\dot\phi_{i,j,k}^{n+1/2}. \tag{25}$$

Here, subscripts refer to the spatial lattice coordinate, superscripts refer to the time coordinate, and $\dot\phi\equiv\partial\phi/\partial\eta$. The spatial grid size will be chosen to be $\Delta x=1$.

In this paper, we will set $\phi_0=1$. The scalar field initial conditions are then chosen using the prescription described above for various bias probabilities, p. That is, in the following we will use percolation theory with allowed field values of ±1 at any lattice site. It is of interest to compare the evolution of the network initialized with two-point initial conditions with those initialized with various continuous distributions. We have done this for a uniform distribution which gives probability $1-p$ of choosing ϕ between -1 and 0 and probability p of choosing between 0 and 1, and with a Gaussian distribution $P(\phi)$ such that $\int_0^{+\infty}d\phi P(\phi)=p$. In general, the surface area of the initial network, measured at $\eta=\eta_0$, is largest in the case of the two-point, percolative distribution. However, after a few steps of dynamical evolution the three networks stabilize, and important characteristics of the network, like surface en-

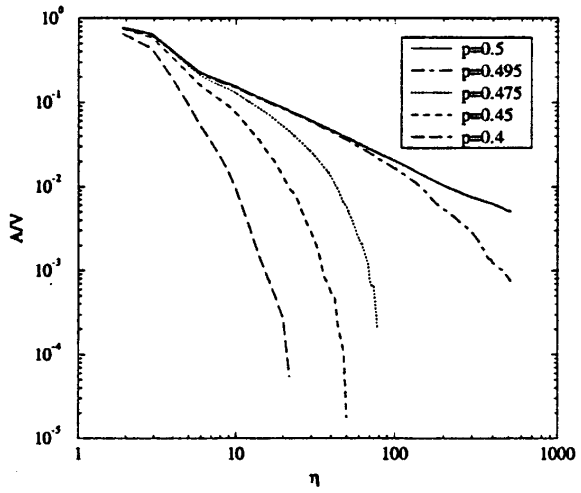

FIG. 7. Evolution of the comoving area, A, of domain walls per volume, V, with conformal time, η, in two dimensional runs. For each bias, p, we show the evolution of one realization.

ergy or kinetic energy and their time evolution, become indistinguishable for a fixed bias p. Hence, the sharp initial conditions of percolation theory also give a good approximation to initial conditions softened by smooth distribution functions. This justifies our use of pure two-point percolation theory initial conditions in this paper.

We will also choose the initial field "velocity" $\dot{\phi}$ to be zero everywhere on the lattice. Again, it is of interest to ask what would happen if we did not choose this condition and allowed nonvanishing initial field velocities. We were able to check that our results were insensitive to the choice of initial velocity by repeating simulations with $\dot{\phi}$ chosen from a uniform distribution of velocities between -1 and $+1$ $[=O(\phi_0/\eta_0)]$.

Simulations were run in the radiation dominated epoch, with $a=(\eta/\eta_0)$ and the initial time, $\eta_0=1$. We chose a wall thickness $w_0=5$, making the ratio $W_0=5$. This value was used to ensure that the wall thickness was well above the lattice resolution scale (recall $\Delta x=1$), while ensuring that for most of the dynamic range of the simulation, the wall-wall separation exceeded the wall thickness.

IV. RESULTS

The focus here is to present the evolution of the energy density of the network of domain walls in the radiation dominated epoch. As each simulation is evolved, the comoving wall area is determined (according to the prescription of PRS) and a plot of this area, A, per comoving volume V versus conformal time is produced.

A. Two-dimensional simulations

Figure 7 shows the evolution of A/V as a function of elapsed conformal time, η, for a number of initial bias probabilities between $p=0.5$ and 0.4. Each simulation ran on a 1024×1024 lattice until either no more domain walls were found in the box, or η exceeded 512 $(=L/2)$.

For the $p=0.5$ case we recover the scaling properties reported in PRS. In this case, a self-similar solution is well established by a time $\eta\sim2w_0$ (that is, after the wall-wall separation well exceeded the wall thickness). Fitting the scaling portion $(10<\eta<100)$ of the curve to the power law

$$A/V\propto\eta^{\bar{\nu}}, \tag{26}$$

we find $\bar{\nu}=-0.88\pm0.04$. This should be compared to the value of $\bar{\nu}=-0.871\pm0.015$ quoted in PRS for a matter dominated universe. Since the physical density ρ varies as $\rho\propto a^{-1}A/V$, we find, from the runs with $p=0.5$,

$$\frac{d\ \ln\rho}{d\ \ln a}=-1.88\pm0.04. \tag{27}$$

Moving away from the $p=0.5$ case, one sees a dramatic departure from self-similar scaling. In each case there is an exponential cutoff in the ratio A/V at some characteristic time. For the cases of p close to 1/2, that is for $p=0.495$, 0.475, and 0.45, we find that the curves are well fitted by a function of the form

$$A/V\propto\eta^{\bar{\nu}}e^{-\eta/\bar{\eta}}. \tag{28}$$

However, for the cases of p near $1-p_c=0.407$, that is, $p=0.425$ and 0.4, a simple exponential suffices:

$$A/V\propto e^{-\eta/\bar{\eta}}. \tag{29}$$

Values for $\bar{\nu}$ and $\bar{\eta}$, averaged over 5 runs for each value of p, are given in Table I. The nonlinear fit to Eq. (28) is made using a least-squares routine with a modified Levenberg-Marquardt algorithm [16]. Recall that in our convention for a radiation dominated universe, $\bar{\eta}=a(\bar{\eta})/a(\eta_0)$. Thus, $\bar{\eta}$ has a physical interpretation as a ratio of the cosmological scale factor when the wall network begins its exponential decay to the scale factor of the initial phase transition.

TABLE I. Fits to the plots of A/V against η for different initial bias probabilities, p, in two dimensions, using the functional forms (28) and (29) given in the text.

p	$\bar{\nu}$	$\bar{\eta}$
0.5	-0.88	–
0.495	-0.82	227
0.475	-0.6	22.4
0.45	-0.68	7.8
0.425	–	3.2
0.4	–	2.2

For p close to 0.5 the domain wall network appears to enter a quasi-scaling regime in which A/V scales $\propto\eta^{\bar{\nu}}$, before eventually being exponentially cutoff at $\eta=\bar{\eta}$. In particular, for the bias $p=0.495$ we see the network scales exactly as the $p=0.5$ case in the epoch $2w_0\leqslant\eta\leqslant60$, before the exponential decay is established. As $p\rightarrow1-p_c=0.407$, however, $\bar{\eta}$ rapidly approaches the resolution size of the grid, and no evidence of early scaling is seen. This behavior continues as p drops below the critical threshold, as indicated in the $p=0.4$ example. We find that for the cases of $p<0.4$ the exponential cutoff of A/V becomes even more

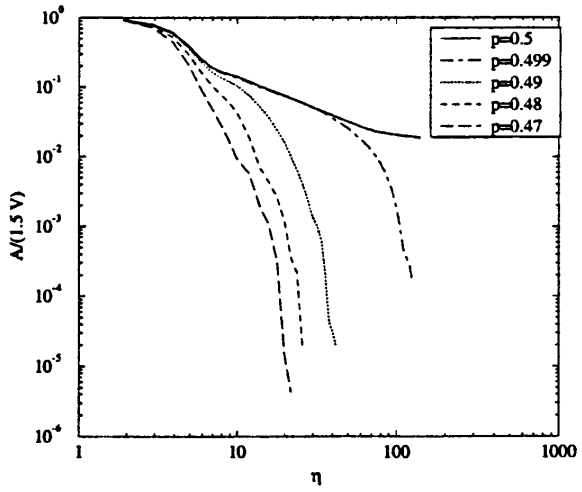

FIG. 8. Evolution of the comoving area, A, of domain walls per volume, V, with conformal time, η, in three-dimensional runs. For each bias, p, we show the evolution of one realization.

precipitous, with the characteristic scale $\bar{\eta}$ rapidly approaching the lattice grid size. We find all of these parameters to be stable to finite grid and time resolution effects; that is, A/V against η plots from runs on $L=512$ and $L=768$ grids overlay those of Fig. 7 exactly, while halving and doubling $\Delta\eta$ have no measurable effect on the parameters of Table I.

The values of $\bar{\nu}$ and $\bar{\eta}$ were found to be only weakly dependent of the value of w_0. Changing the wall thickness affects the network evolution through two closely balanced effects. Increasing the height of the potential barrier between the two vacua makes transition from one vacuum to the other energetically less favorable. But, this is compensated somewhat by the increased domain wall surface tension. However, for a quartic potential, the value of V_0 clearly does not scale out of the equations of motion, so this balance need not be exact. (In the domain wall scenario, the scalar field is off the vacuum manifold at many points throughout space, making the evolution more dependent on the relative values of V_0 and ϕ_0 than, say, a texture scenario, where the nonlinear σ model works well [17], and evolution is effectively independent of the potential barrier between vacua.)

To conclude, in the two-dimensional simulations we see persistent scaling behavior precisely at $p=0.5$. For p below 0.5 but above the critical threshold $1-p_c=0.407$, we see scaling for a finite time which is then exponentially cutoff at some conformal time $\bar{\eta}$. The value of $\bar{\eta}$, which becomes very large as $p\to 0.5$, decreases rapidly as p approaches the critical threshold. Near $p=0.407$, and below it, no scaling behavior is seen and the behavior is well described by a simple exponential for all conformal time.

B. Three-dimensional simulations

The three-dimensional simulations are run on a 128^3 grid. They were run until a time $\eta=128(=L)$, or until no more walls remained in the box. The domain wall thickness was again set to $w_0=5$, leaving us with only modest dynamic range in which to follow the network evolution.

A plot of A/V for these runs is shown in Fig. 8. Again, the self-similar evolution seen in PRS for the $p=0.5$ case is reproduced well in the time range $2w_0<\eta<L/2$. Measuring the logarithmic slope of A/V versus η between these times we find $\bar{\nu}=-0.89\pm0.06$. This is to be compared with the value found in PRS of $\bar{\nu}=-0.92\pm0.06$ for their three-dimensional simulations in a matter-dominated epoch.

TABLE II. Fits to the plots of A/V against η for different initial bias probabilities, p, in three dimensions using the functional form (29) given in the text. For the $p=0.499$ case we report the best fit to Eq. (29), although the late-time decay was found to be somewhat steeper than an exponential.

p	$\bar{\nu}$	$\bar{\eta}$
0.5	−0.89	–
0.499	−0.43	38.7
0.49	–	5.4
0.48	–	2.8
0.47	–	1.8

With $p\neq 0.5$, we see qualitative features in the three-dimensional runs similar to those of the two-dimensional cases. The one major difference is that the turnover into an exponential decay is seen to occur much earlier, so much so in fact that all but one of the cases considered here ($p=0.47,0.48,0.49$) are well fitted by a simple exponential curve with no initial pseudoscaling regime. Using a fitting function of the form of Eq. (29), the values of the $\bar{\eta}$ for each p are given in Table II.

To demonstrate the presence of an early scaling regime in three dimensions we also considered the fine-tuned case of $p=0.499$. The evolution of the wall surface area in this case follows that of the scaling $p=0.5$ case closely until a time $\eta\simeq 30$, after which the area decays rapidly. In this case the decay was found to be considerably steeper than the exponential tail of Eq. (28) could accommodate.

To conclude, in the three-dimensional case we see persistent scaling behavior precisely at $p=0.5$. A pseudoscaling regime is seen for biases close to $p=0.5$, but for $p\leqslant 0.49$, little or no scaling is observed and the behavior is well described by a simple exponential for all conformal time.

C. Discussion of modifications to the equations of motion

Following PRS, we ran one simulation setting the values of the parameters α and β to reproduce the original equation of motion, Eq. (5). In this run, the domain walls maintained a constant physical rather than comoving thickness, and so problems of available dynamic range become important. The prescription used was as follows.

The simulation was run on a 512×512 lattice, with our standard field initial conditions and $p=0.5$. Using a wall thickness of $w_0=25$, the initial conditions were evolved with the standard parameter values of $\alpha=3$ and $\beta=0$, until a time when the wall-wall separation exceeded the wall thickness; that is, a time $\eta=2w_0$. The equation of motion was then changed, to set $\alpha=\beta=2$ until a time $\eta=250$. The comoving thickness of the walls at the end of the simulation was then 5 lattice sites.

To compare, the run was repeated, this time leaving the standard parameter values fixed throughout the simulation. The two plots of surface area versus η are shown in Fig. 9.

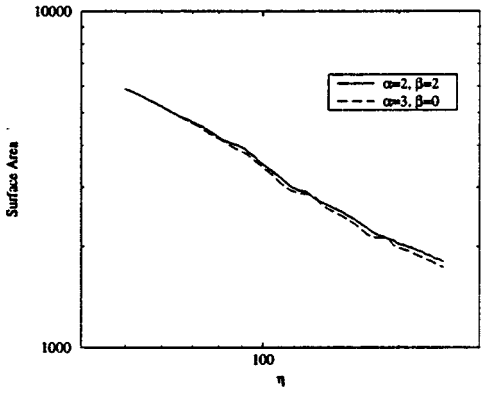

FIG. 9. Comparison of the evolution of the domain wall network with equations of motion which preserve physical ($\alpha=\beta=2$) and comoving ($\alpha=3$, $\beta=0$) wall thickness. The units of the surface area axis are arbitrary.

As discussed in PRS, we do not have the dynamic range available to see clear self-similar scaling in this thick wall limit. However, Fig. 9 does clearly show that the evolution of the walls of constant physical thickness (that is, those following the true scalar field equations of motion) does match well that of the walls of constant comoving thickness.

We can further note that in the case of the piecewise quadratic potential, 9, the linear equations of motion can be solved. In the oscillatory regime in which $\phi_k \sim \pm\phi_0$, and $V(\phi)\sim(|\phi|-\phi_0)^2$ one can show that the solutions for ϕ_k with $\alpha=\beta=2$ and $\alpha=3$, $\beta=0$ have the same form, with

$$\langle(|\phi_k|-\phi_0)^2\rangle \sim \frac{1}{\eta^3}. \tag{30}$$

V. DISCUSSION

In our numerical experiments we have considered initial domain wall networks constructed from a scalar field set at each spatial point to one of two discrete values of a $\mathcal{Z}_2$ vacuum manifold. Such a distribution is described exactly by percolation theory, thus giving us analytical insight into the nature of these initial networks. We have shown that during the dynamical evolution of such initial conditions, all interesting quantities rapidly converge to those given by other continuous distributions. It follows that the time evolved results given in this paper are valid for a generic set of physical conditions which initialize the vacuum structure.

By considering the exactly solvable case of a piecewise quadratic potential we have seen that for the case of an initially biased phase transition, $p\neq 0.5$, with degenerate vacua, one vacuum will come to dominate all space. Our numerical results confirm this in the case of a more generic nonlinear scalar field evolution.

In the two-dimensional runs we found that for $p=0.5$ there was long-term scaling behavior. In the range $0.5>p>0.45$ the energy density of the network entered an early ''pseudoscaling'' regime, before cutting off exponentially. For $p<0.45$ only exponential decay was seen.

The topology of the initial domain wall network fell into two classes. For those cases with $p<0.407$, the critical probability, one sees only isolated ''bags'' of one vacuum in a ''sea'' of the other percolating vacuum. Once the horizon becomes comparable to the typical size of one of these bags they rapidly decay under their surface tension, and the network energy density in these cases is seen to go rapidly to zero. This underlies the exponential decay behavior observed in the domain wall surface area. For $0.5\geqslant p>0.407$ neither vacuum percolates in two dimensions, and so a complicated tangle of domain walls form. For $p=0.5$ no one vacuum can dominate, and the delicate balance of the zero mode of the scalar field at $\phi_{(k=0)}=0$ leads to a long-term scaling. For the cases $0.5>p>0.407$ the initial tangle of domain walls slowly breaks down into a collection of bags of the less dominant vacuum, and these eventually (at a time $\eta\simeq\bar{\eta}$) collapse under their surface tension.

In three dimensions the nature of the initial conditions is qualitatively different, although the evolution of these initial wall networks leads to very similar behavior. For the cases with $p<0.311$, the critical threshold, only one vacuum percolates the lattice, and so, once more, isolated bags of one vacuum are to be found in a percolating sea of the more dominant vacuum. Again, these bags rapidly decay under their surface tension.

For the cases of $p>0.311$, both vacua percolate in three dimensions. We have seen that this leads to an initial network of infinite (lattice sized) domain walls. For $p=0.5$ there was long-term scaling behavior. However, we find that the decay of the wall energy density for $0.5>p>0.311$ in three dimensions is more acute than that in two dimensions. In these cases the initial infinite domain walls are forced to rapidly decompose into vacuum bags which then decay. Only in the range $0.49\leqslant p\leqslant 0.5$ is long-term scaling seen.

We have shown that domain walls come to dominate the energy density of the universe only in the case of $p=0.5$. Domain walls formed in a biased phase transition will necessarily have only a finite effective lifetime. This allows for the possibility of cosmologically interesting domain wall scenarios which evade current observational restrictions, such as the tight limits on the anisotropy of the microwave background. One such scenario is a network of domain walls forming well before matter-radiation equality, with a bias close to $p=0.5$, so that the network decays before photon decoupling (at a redshift $z\simeq 1000$). Such walls would be sufficiently massive to contribute significantly to large scale structure formation on comoving scales less than ~ 20 Mpc (the horizon at decoupling), but would decay before photon last scattering, and hence not contribute to the large scale cosmic microwave background anisotropy [18]. Such a scenario might be workable, for example, in a universe dominated by hot dark matter in conjunction with scale invariant primordial perturbations induced by an earlier inflationary epoch. In such a scenario, the early domain wall network would add small scale power in the matter distribution, as required by current observations.

Unfortunately, for much of the range of biases, we find that the domain wall networks are likely to be cosmologically innocuous. Their energy density exponentially decays with a characteristic time scale of only a few expansion times. In order to see any significant scaling of the network before the ultimate exponential decay seems to require some degree of fine tuning of p close to 1/2.

ACKNOWLEDGMENTS

We thank Paul Steinhardt, Rob Crittenden, and David Spergel for their useful comments. The work of D.C. was supported by the DOE under Contract No. DOE-EY-76-C-02-3071, while that of Z.L. and B.O. was supported in part by the DOE under Contract No. DOE-AC02-76-ERO-3071 and NATO Contract Ref. CRG 940784. Z.L. was also partially supported by Polish Committee for Scientific Research.

[1] For review see, for example, A. Liddle and D. Lyth, Phys. Rep. **231**, 1 (1993).
[2] Y.B. Zel'dovich, I.Y. Kobzarev, and L.B. Okun, Sov. Phys. JETP **40**, 1 (1975).
[3] T. Kibble, J. Phys. A **9**, 1387 (1976).
[4] D. Spergel and N. Turok, Phys. Rev. Lett. **64**, 2736 (1990).
[5] A. Albrecht, D. Coulson, P. Ferreira, and J. Magueijo, Phys. Rev. Lett. **76**, 1413 (1996).
[6] D. Coulson, P. Ferreira, P. Graham, and N. Turok, Nature (London) **368**, 27 (1994); R. Crittenden and N. Turok, Phys. Rev. Lett. **75**, 2642 (1995).
[7] I. Wasserman, Phys. Rev. Lett. **57**, 2234 (1986); C. Hill, D. Schramm, and J. Fry, Comments Nucl. Part. Phys. **19**, 25 (1989).
[8] C. Hill and G. Ross, Nucl. Phys. **B331**, 253 (1988); Phys. Lett. B **203**, 125 (1988); A. Gupta, C. Hill, R. Holman, and E. Kolb, Phys. Rev. D **45**, 441 (1992).
[9] W. Press, B. Ryden, and D. Spergel, Astrophys. J. **347**, 590 (1989).
[10] L. Kawano, Phys. Rev. D **41**, 1013 (1990).
[11] B. Ovrut and S. Thomas, Phys. Lett. B **277**, 53 (1992); **257**, 292 (1991); **267**, 227 (1991); E.W. Kolb and Y. Wang, Phys. Rev. D **45**, 4421 (1992).
[12] M. Sykes, D. Gaunt, and M. Glen, J. Phys. A **9**, 1705 (1976); A. Flammang, Z. Phys. B **22**, 47 (1977).
[13] Z. Lalak, B. Ovrut, and S. Thomas, Phys. Rev. D **51**, 5456 (1995).
[14] Z. Lalak and B. Ovrut (in preparation).
[15] D. Stauffer, Phys. Rep. **54**, 1 (1979); A. Aharony, in *Directions in Condensed Matter Physics*, edited by G. Grinstein and G. Mazenko (World Scientific, Singapore, 1986).
[16] W. Press, S. Teukolsky, W. Vetterling, and B. Flannery, *Numerical Recipes* (Cambridge University Press, Cambridge, England, 1992).
[17] U.L. Pen, D. Spergel, and N. Turok, Phys. Rev. D **49**, 692 (1994).
[18] Z. Lalak, S. Lola, B. Ovrut, and G.G. Ross, Nucl. Phys. **B434**, 675 (1995).